

Supporting Information

Experimental Design of (Cs,Rb)₂Sn(Bi)Cl₆ Blue Phosphors by Cation-Substitution-Induced Lattice Strain

**Oleksandr Stroyuk^{1*}, Oleksandra Raievska¹, Manuel Daum^{1,2},
Christian Kupfer¹, Andres Osvet², Jens Hauch^{1,2}, Christoph J. Brabec^{1,2}**

¹*Forschungszentrum Jülich GmbH, Helmholtz-Institut Erlangen Nürnberg für Erneuerbare Energien
(HI ERN), 91058 Erlangen, Germany*

²*Friedrich-Alexander-Universität Erlangen-Nürnberg, Materials for Electronics and Energy Technology (i-MEET),
Martensstrasse 7, 91058 Erlangen, Germany*

Authors for correspondence:

*Dr. Oleksandr Stroyuk, Forschungszentrum Jülich GmbH, Helmholtz-Institut Erlangen Nürnberg für Erneuerbare Energien (HI ERN), Immerwahrstr. 2, 91058 Erlangen, Germany; *e-mail*: o.stroyuk@fz-juelich.de, alstroyuk@ukr.net.

Materials and Methods

Synthesis of (Cs_xRb_{1-x})₂Sn_yBi_{1-y}Cl₆ samples

Preparation of stock solutions.

1.0 M SnCl₄ solution in aqueous 4.0 M HCl solution: 3.506 g SnCl₄·5H₂O were dissolved in 3.3 mL of 12 M (37%) aqueous HCl solution and diluted with deionized (DI) water up to a total volume of 10 mL.

1.0 M BiCl₃ solution in aqueous 4.0 M HCl solution: 3.153 g BiCl₃ were dissolved in 3.3 mL of 12 M (37%) aqueous HCl and diluted with DI water to a total volume of 10 mL.

1.0 M aqueous CsCl solution: 1.683 g CsCl is dissolved in 9.0 mL of DI water and diluted with DI water to a total volume of 10 mL.

1.0 M aqueous Rb acetate (ac) solution: 1.445 g RbAc is dissolved in 9.0 mL of DI water and diluted with DI water to a total volume of 10 mL.

Acidic water/2-propanol mixture: 0.05 mL of 12 M aqueous HCl solution is mixed with 0.95 mL of 2-propanol.

Preparation of precursor solutions.

Precursor #1: 0.1 mL of 1.0 M aqueous solution of metal chlorides ($\text{SnCl}_4 + \text{BiCl}_3$) in 4.0 M HCl is mixed with 1.0 mL of a solution containing 0.05 mL of 12 M (37%) aqueous HCl and 0.95 mL of 2-propanol.

Precursor #2: 0.5 mL of 2-propanol is added to 0.25 mL of 1.0 M aqueous solution of monovalent metal salts ($\text{CsCl} + \text{RbAc}$). The monovalent metal cations are taken in a 25% excess with respect to the stoichiometry (250 μL of 1.0 M solution instead of 200 μL) to facilitate precipitation of the final perovskite products, which is partially soluble in water/2-propanol mixture. In this way, the reaction yield is increased.

Preparation of precursor plates.

Manual or robot-assisted combinatorial synthesis is performed by mixing reactants from two precursor plates produced from corresponding precursor solutions. The stock solutions are introduced into 2-mL Eppendorf vials fixed in the form of a 6 \times 8 sample plate, at intense stirring on a shaking unit of the Tecan pipetting robot (see more details in Ref. [17] and corresponding SI). After two precursor plates are produced, the solutions from precursor plate #2 are transferred by the pipetting robot into corresponding vials of precursor plate #1 according to the number of wells. The mixing of the solutions in vials is performed under intense shaking.

Precursor plate #1 contains 6 identical horizontal rows of samples, 8 samples per row numbered 1 through 8. The composition of the samples with corresponding well numbers is presented below.

Well 1: 100 μL of 1.0 M aqueous SnCl_4 (4.0 M HCl), no BiCl_3 , 1.0 mL of solution containing 0.05 mL aqueous 12 M (37%) HCl and 0.95 mL of 2-propanol.

Well 2: 95 μL of 1.0 M aqueous SnCl_4 (4.0 M HCl), 5 μL of aqueous BiCl_3 (4.0 M HCl), 1.0 mL of solution containing 0.05 mL aqueous 12 M (37%) HCl and 0.95 mL of 2-propanol.

Well 3: 90 μL of 1.0 M aqueous SnCl_4 (4.0 M HCl), 10 μL of aqueous BiCl_3 (4.0 M HCl), 1.0 mL of solution containing 0.05 mL aqueous 12 M (37%) HCl and 0.95 mL of 2-propanol.

Well 4: 75 μL of 1.0 M aqueous SnCl_4 (4.0 M HCl), 25 μL of aqueous BiCl_3 (4.0 M HCl), 1.0 mL of solution containing 0.05 mL aqueous 12 M (37%) HCl and 0.95 mL of 2-propanol.

Well 5: 50 μL of 1.0 M aqueous SnCl_4 (4.0 M HCl), 50 μL of aqueous BiCl_3 (4.0 M HCl), 1.0 mL of solution containing 0.05 mL aqueous 12 M (37%) HCl and 0.95 mL of 2-propanol.

Well 6: 25 μL of 1.0 M aqueous SnCl_4 (4.0 M HCl), 75 μL of aqueous BiCl_3 (4.0 M HCl), 1.0 mL of solution containing 0.05 mL aqueous 12 M (37%) HCl and 0.95 mL of 2-propanol.

Well 7: 10 μL of 1.0 M aqueous SnCl_4 (4.0 M HCl), 90 μL of aqueous BiCl_3 (4.0 M HCl), 1.0 mL of solution containing 0.05 mL aqueous 12 M (37%) HCl and 0.95 mL of 2-propanol.

Well 8: no SnCl_4 , 100 μL of aqueous BiCl_3 (4.0 M HCl), 1.0 mL of precursor solution containing 0.05 mL aqueous 12 M (37%) HCl and 0.95 mL of 2-propanol.

Precursor plate #2 contains 6 identical vertical columns of samples, 6 samples per column marked as "A" through "F". The composition of the samples with corresponding well markings is presented below.

Well A: 250 μL of 1.0 M aqueous CsCl, no RbAc, 500 μL of 2-propanol.

Well B: 200 μL of 1.0 M aqueous CsCl, 50 μL of 1.0 M aqueous RbAc, 500 μL of 2-propanol.

Well C: 150 μL of 1.0 M aqueous CsCl, 100 μL of 1.0 M aqueous RbAc, 500 μL of 2-propanol.

Well D: 100 μL of 1.0 M aqueous CsCl, 150 μL of 1.0 M aqueous RbAc, 500 μL of 2-propanol.

Well E: 50 μL of 1.0 M aqueous CsCl, 200 μL of 1.0 M aqueous RbAc, 500 μL of 2-propanol.

Well F: no CsCl, 250 μL of 1.0 M aqueous RbAc, 500 μL of 2-propanol.

Combinatorial synthesis and purification.

The synthesis of $(\text{Cs}_x\text{Rb}_{1-x})_2\text{Sn}_y\text{Bi}_{1-y}\text{Cl}_6$ compounds is performed by mixing corresponding wells of both precursor plates, either manually or with the Tecan pipetting robot. In a typical procedure, solutions from precursor plate #2 are added to corresponding wells of precursor plate #1 at intense shaking. The precipitates form immediately upon mixing and then the samples are kept under shaking for 5 min. No additional thermal treatments are applied

The resulting suspension is left without stirring for 12-14 to complete crystallization. After that, the suspensions are subjected to centrifugation at 1500 rpm for 2 min, and the precipitates are separated from corresponding supernatants. The precipitates are mixed with 1 mL of 2-propanol and shaken till the formation of homogeneous suspensions, centrifuged, and separated from the supernatant. This purification procedure is repeated once again.

Preparation of samples for spectral and structural characterizations.

Freshly prepared and purified precipitates are mixed with 0.2 mL of 2-propanol and refluxed till the formation of homogeneous suspensions. 0.05 mL of such suspensions are deposited on a 1 cm^2 glass substrate or a circular well of plastic Eppendorf 6 \times 8 plate (see photographs in Figure S4). The deposits are left for complete solvent evaporation and used then for spectral measurements and powder X-ray diffraction studies. To prepare samples for scanning electron microscopy, the suspensions are deposited on pieces of two-sided sticky carbon tape arranged on a silicon substrate in the form of a 6 \times 8 sample array.

Instrumental methods

X-ray diffraction (XRD) patterns were registered using a Panalytical X'pert powder diffractometer with filtered Cu K_{α} radiation ($\lambda = 1.54178 \text{ \AA}$) and an X'Celerator solid-state stripe detector in the Bragg-Brentano geometry in an angle range of $2\theta = 5\text{-}100^{\circ}$ with a step rate of 0.05° per min.

The XRD patterns were subjected to a Rietveld refinement procedure using MAUD software (version 2.99). Structural CIF files were downloaded from the Crystallography Open Database (COD, <https://www.crystallography.net/cod/>).

Scanning electron microscopy (SEM) imaging and energy-dispersive X-ray spectroscopic (EDX) analysis were performed using a JEOL JSM-7610F Schottky field emission scanning electron microscope operating under 15-20 kV acceleration voltage and equipped with an X-Max 80 mm² silicon drift detector (Oxford Instruments) and AZtec nanoanalysis software. EDX spectra were collected for at least four different spots of each sample and the results were averaged.

Raman spectra were registered on a WITec alpha700 confocal Raman microscope equipped with a UHTS 300 spectrometer and a 532-nm laser.

Reflectance spectra were recorded using a BlackComet spectrometer (StellarNet Inc.) and a 75 W Xenon lamp (Thorlabs) as an excitation source. The spectra were registered with an optical Y-fiber probe in identical geometry for samples and a scattering reference (ultra-pure BaSO₄, Alfa-Aesar). The reflectance spectra were transformed into absorption spectra using the Kubelka-Munk formula and the reference.

Absolute PL QYs were determined using a Quantaaurus-QY spectrometer (Hamamatsu) at room temperature. The sample was excited by the light from an in-built Xenon lamp with an excitation wavelength selected using a monochromator with a 5-nm spectral width. Ultra-pure BaSO₄ from Sigma-Aldrich was used as scattering references, all producing identical results. Three independently synthesized samples with the same composition were measured with a set of different excitation wavelengths varied from 290 to 410 nm.

Photoluminescence (PL) and PL excitation (PLE) spectra were collected using a plate-reading spectrometer integrated into the Tecan pipetting robot. PL was excited at 345 nm, PLE signal registered at 475 nm. The PL spectra were found to be identical to those registered during PL QY measurements using the Quantaaurus spectrometer.

Temperature dependences of PL spectra were collected using an Optistat DN-X cryostat (Oxford Instruments) controlled by a MercuryITC temperature controller (Oxford Instruments) in the range of 80-340 K. The samples were drop-cast as suspensions in 2-propanol on glass and dried at ambient conditions. The series of PL spectra at different temperatures were collected three times, yielding identical results.

Kinetic curves of PL decay were registered using a custom-designed setup based on a FluoTime300 luminescence spectrometer (Picoquant) equipped with a 402 nm LDH-P-C-405B laser. The samples were excited by the 402 nm laser using an optical fiber and the PL signal was collected in the range of 420-800 nm with excitation and emission slits set to 4 nm.

Photographs of luminescent samples were registered at ambient conditions under illumination with a UV lamp (350-370 nm).

Microstrain–size analysis using MAUD software.

Rietveld refinement of the XRD patterns yields several fitting parameters that can be analyzed as functions of the sample composition (x and y), including lattice parameters as well as grain size and residual lattice microstrain. Both size and strain are simultaneously derived by MAUD software from the inhomogeneous broadening of the diffraction peaks using the approach of Lutterotti and Scardi [s1] for the case of homogeneous strain distribution. In this approach, the shape of the peak is described by a pseudo-Voigt function (pV) that can be resolved into a system of equations with the grain size D and the mean square of the lattice microstrain $\langle \varepsilon^2 \rangle$:

$$Z = \eta / (1 - \eta) (\pi / \ln 2)^{1/2} \quad (1)$$

$$Z / (Z + 1) \times \exp[-(Z + 1)^2 / (16 \ln 2)] + 1 / (Z + 1) \times \exp[-(Z + 1) / 2] = \exp(-\pi^2 \langle \varepsilon^2 \rangle D^2 / (2L^2) - 1/2) \quad (2)$$

$$\text{HWHM} = \arcsin[\lambda(Z + 1) / (4\pi D) + \sin \theta_0] - \theta \quad (3)$$

where HWHM – is half width at half maximum of pV function, η – Gaussian content of pV; L – lattice parameter; λ – X-ray wavelength, θ_0 – Bragg angle of K_α peak.

Taking D and $\langle \varepsilon^2 \rangle$ as fitting parameters, MAUD performs an iterative search for the best reproduction of the peak shape for the given HWHM and η .

[s1]. L. Lutterotti, P. Scardi, Simultaneous Structure and Size-Strain Refinement by the Rietveld Method, J. Appl. Cryst., 1990, 23, 246-252.

Equations

Temperature dependence of integral PL intensity $I(T)$:

$$I(T) = \frac{I_0}{1 + \text{const} \times \exp(-E_b/k_b T)} \quad (\text{S1}).$$

Here, I_0 is the PL intensity at $T = 0$, E_b is a potential barrier of free-to-self-trapped excitonic transition, and k_b is the Boltzmann constant.

Temperature dependence of the spectral width (Full Width on Half Maximum, FWHM) of PL band:

$$\text{FWHM}(T) = 2.36\sqrt{S}E_{ph}\sqrt{\cot\left(\frac{E_{ph}}{2k_b T}\right)} \quad (\text{S2}).$$

Here, S is the Huang-Rhys factor, and E_{ph} is phonon energy.

A stretched exponential function used for fitting PL decay curves:

$$I(t) = I_0 \exp\left(\left(-\frac{t}{\tau_{PL}}\right)^{\frac{1}{h}}\right) \quad (\text{S3}).$$

Here, I_0 and I are initial ($t = 0$) and current PL intensity, h is the heterogeneity factor, and τ_{PL} is the average PL lifetime (h and τ are fitting parameters).

Equations for rate constants of radiative (k_r) and non-radiative (k_{nr}) recombination:

$$k_r = \frac{\text{PL QY}}{\tau_{PL}} \quad (\text{S4}),$$

$$\tau_{PL} = \frac{1}{k_r + k_{nr}} \quad (\text{S5}).$$

Tables

Table S1. The nominal and actual composition of $\text{Cs}_2\text{Sn}(\text{Bi})\text{Cl}_6$ samples

Sample	Nominal Bi fraction	Actual Bi fraction	Cl/(Sn+Bi)	Cs/(Sn+Bi)	Cl/Cs
A1	0	0	4.9	1.9	2.7
A2	0.05	0.08	4.8	1.9	2.7
A3	0.10	0.12	4.7	1.9	2.6
A4	0.25	0.24	4.7	1.8	2.5
A5	0.50	0.46	4.6	2.0	2.4
A6	0.75	0.75	4.5	2.0	2.2
A7	0.90	0.82	4.4	2.2	2.1
A8	1.00	1.00	4.4	2.6	1.7

Notes: The accuracy of determination by EDX is ± 0.01 for actual Bi fraction and ± 0.1 for Cl/(Sn+Bi), Cs/(Sn+Bi), and Cl/Cs ratios.

Table S2. The nominal compositions of $(\text{Cs}_x\text{Rb}_{1-x})_2\text{Sn}_y\text{Bi}_{1-y}\text{Cl}_6$ products produced by the robot-assisted HTP synthesis

	1	2	3	4	5	6	7	8
A	$x = 1.0$ $y = 1.00$	$x = 1.0$ $y = 0.95$	$x = 1.0$ $y = 0.90$	$x = 1.0$ $y = 0.75$	$x = 1.0$ $y = 0.50$	$x = 1.0$ $y = 0.25$	$x = 1.0$ $y = 0.10$	$x = 1.0$ $y = 0$
B	$x = 0.8$ $y = 1.00$	$x = 0.8$ $y = 0.95$	$x = 0.8$ $y = 0.90$	$x = 0.8$ $y = 0.75$	$x = 0.8$ $y = 0.50$	$x = 0.8$ $y = 0.25$	$x = 0.8$ $y = 0.10$	$x = 0.8$ $y = 0$
C	$x = 0.6$ $y = 1.00$	$x = 0.6$ $y = 0.95$	$x = 0.6$ $y = 0.90$	$x = 0.6$ $y = 0.75$	$x = 0.6$ $y = 0.50$	$x = 0.6$ $y = 0.25$	$x = 0.6$ $y = 0.10$	$x = 0.6$ $y = 0$
D	$x = 0.4$ $y = 1.00$	$x = 0.4$ $y = 0.95$	$x = 0.4$ $y = 0.90$	$x = 0.4$ $y = 0.75$	$x = 0.4$ $y = 0.50$	$x = 0.4$ $y = 0.25$	$x = 0.4$ $y = 0.10$	$x = 0.4$ $y = 0$
E	$x = 0.2$ $y = 1.00$	$x = 0.2$ $y = 0.95$	$x = 0.2$ $y = 0.90$	$x = 0.2$ $y = 0.75$	$x = 0.2$ $y = 0.50$	$x = 0.2$ $y = 0.25$	$x = 0.2$ $y = 0.10$	$x = 0.2$ $y = 0$
F	$x = 0$ $y = 1.00$	$x = 0$ $y = 0.95$	$x = 0$ $y = 0.90$	$x = 0$ $y = 0.75$	$x = 0$ $y = 0.50$	$x = 0$ $y = 0.25$	$x = 0$ $y = 0.10$	$x = 0$ $y = 0$

Figures

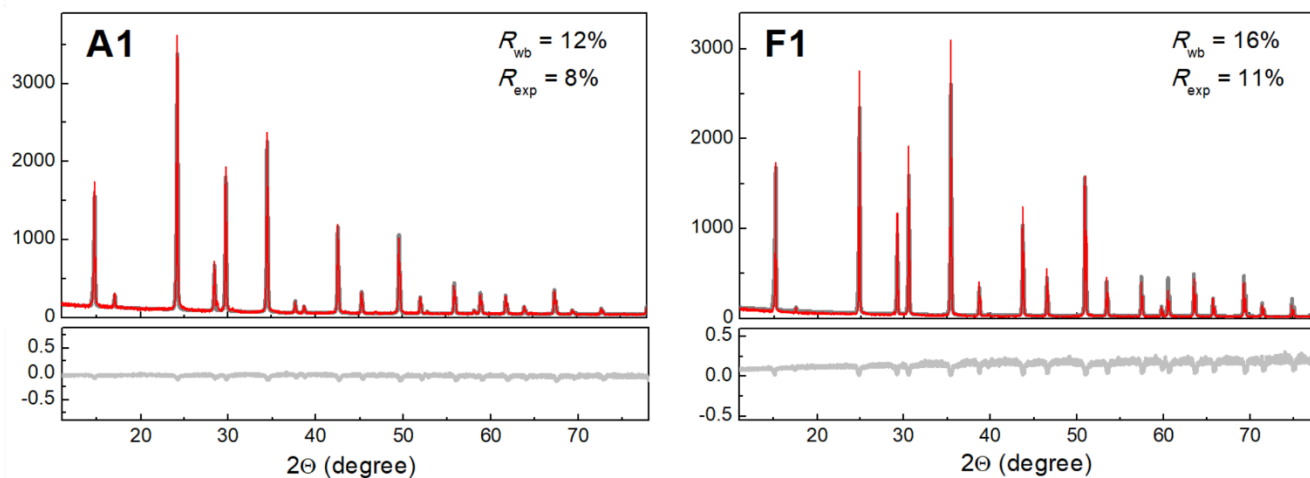


Figure S1. Examples of Rietveld refinement of A1 and F1 samples showing experimental and calculated XRD profiles (upper panels, gray and red solid lines, respectively), fitting residuals (lower panel, light-gray solid lines), and fit quality parameters, R_{wb} and R_{exp} .

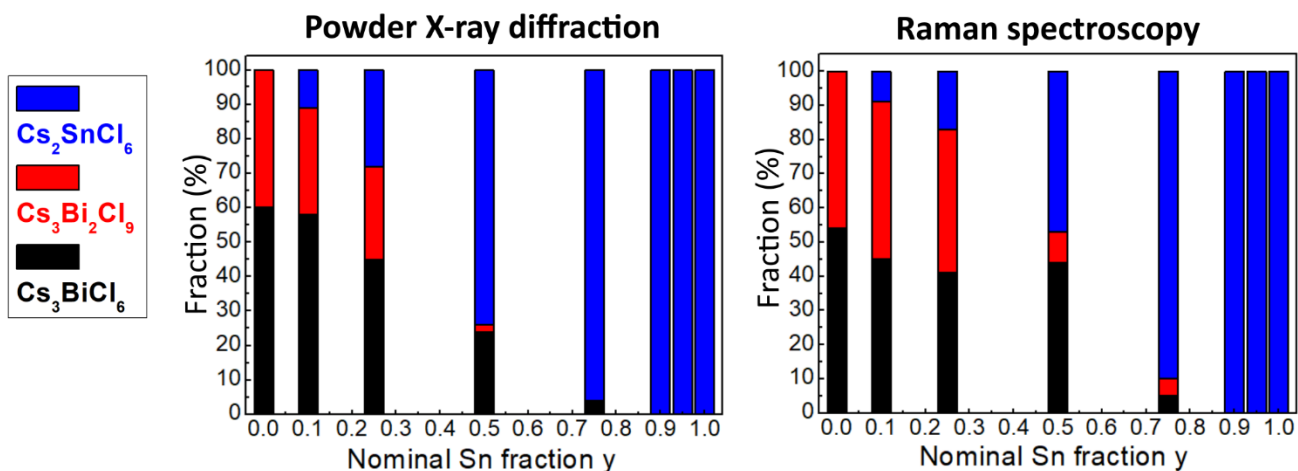


Figure S2. Fractions of different phases found in $\text{Cs}_2\text{Sn}_y\text{Bi}_{1-y}\text{Cl}_6$ products with varied nominal y by Rietveld refinement of XRD patterns and multi-Lorentzian fitting of Raman spectra.

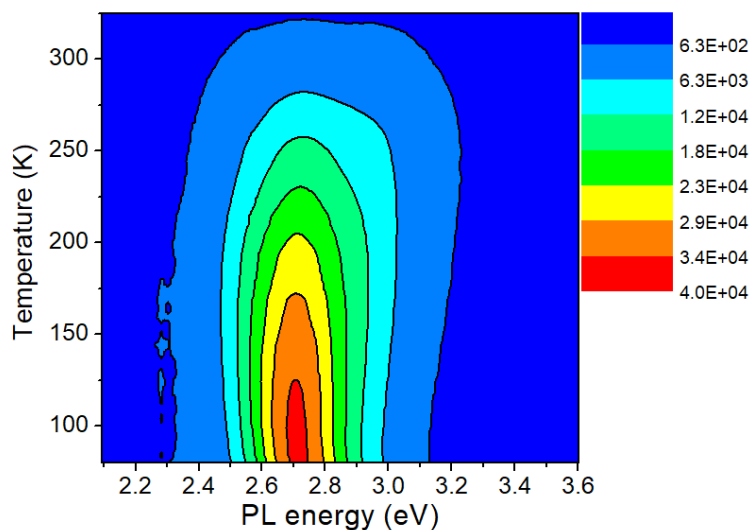


Figure S3. Spectral map showing the evolution of PL emission with temperature in the range of 80-325 K varied with a step of 5 K.

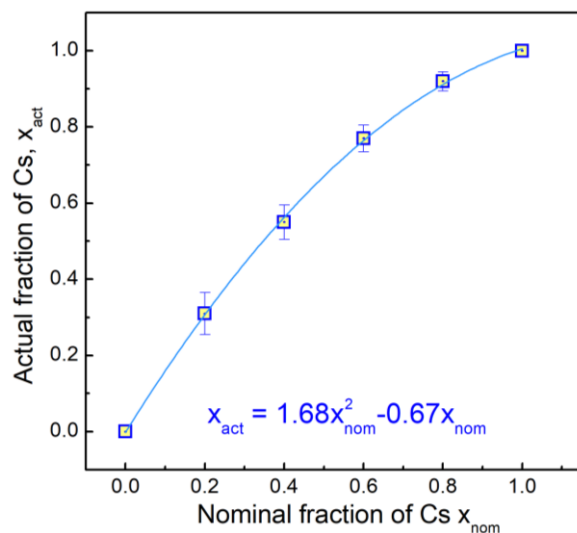


Figure S4. Relationship between nominal (x_{nom}) and actual (x_{act}) molar fraction of Cs in $(Cs_xRb_{1-x})_2SnCl_6$ perovskites. The solid line represents polynomial fit resulting in $x_{act}(x_{nom})$ equation presented in the figure.

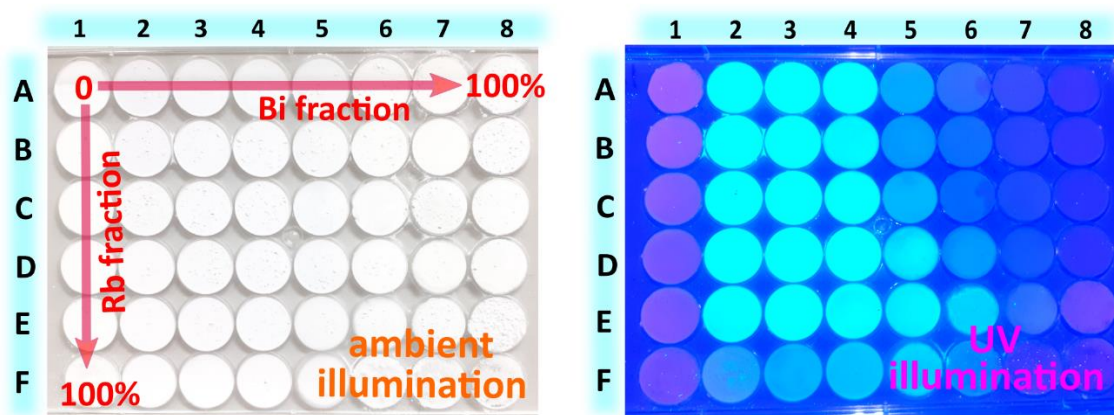


Figure S5. Photographs of $(Cs_xRb_{1-x})_2Sn_yBi_{1-y}Cl_6$ sample plate registered under ambient and UV (370-390 nm) illumination.

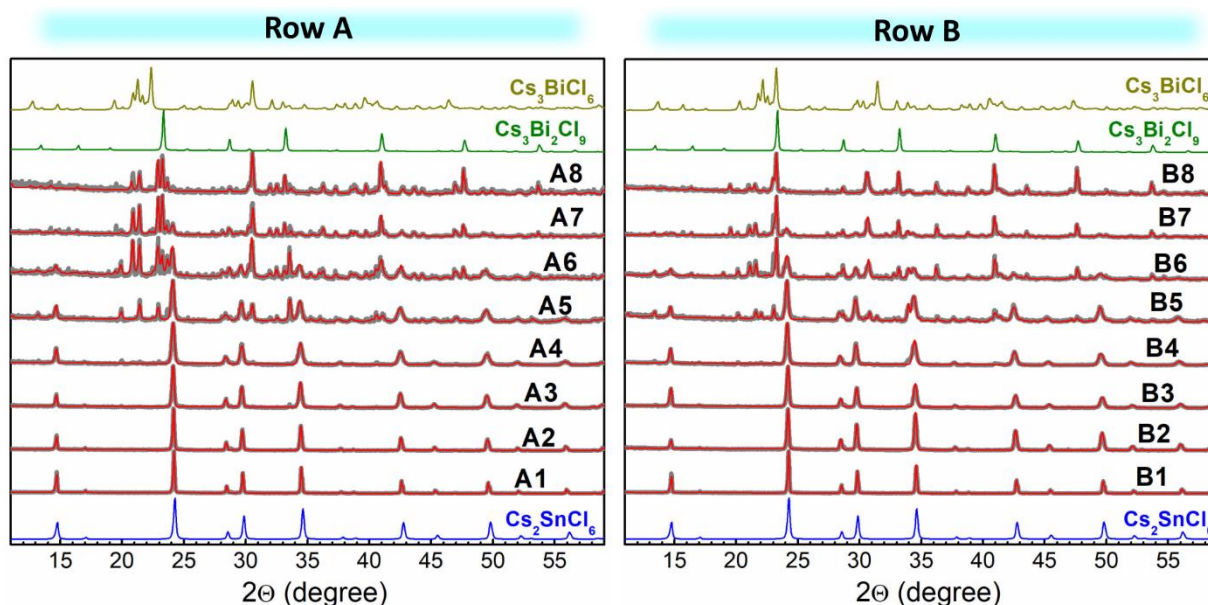


Figure S6. Powder X-ray diffraction patterns of $(\text{Cs}_x\text{Rb}_{1-x})_2\text{Sn}_y\text{Bi}_{1-y}\text{Cl}_6$ products in rows A and B. Gray lines show experimental diffractograms, red lines – Rietveld refinement. Calculated XRD profiles of single phases used for the refinements are presented along with experimental data.

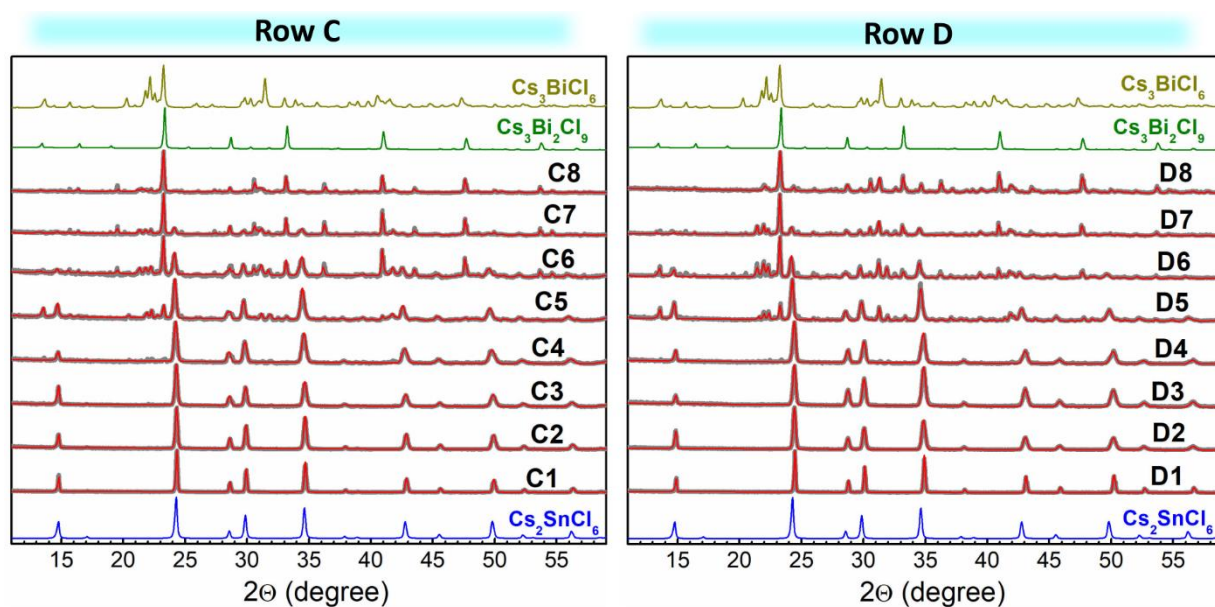


Figure S7. Powder X-ray diffraction patterns of $(\text{Cs}_x\text{Rb}_{1-x})_2\text{Sn}_y\text{Bi}_{1-y}\text{Cl}_6$ products in rows C and D. Gray lines show experimental diffractograms, red lines – Rietveld refinement. Calculated XRD profiles of single phases used for the refinements are presented along with experimental data.

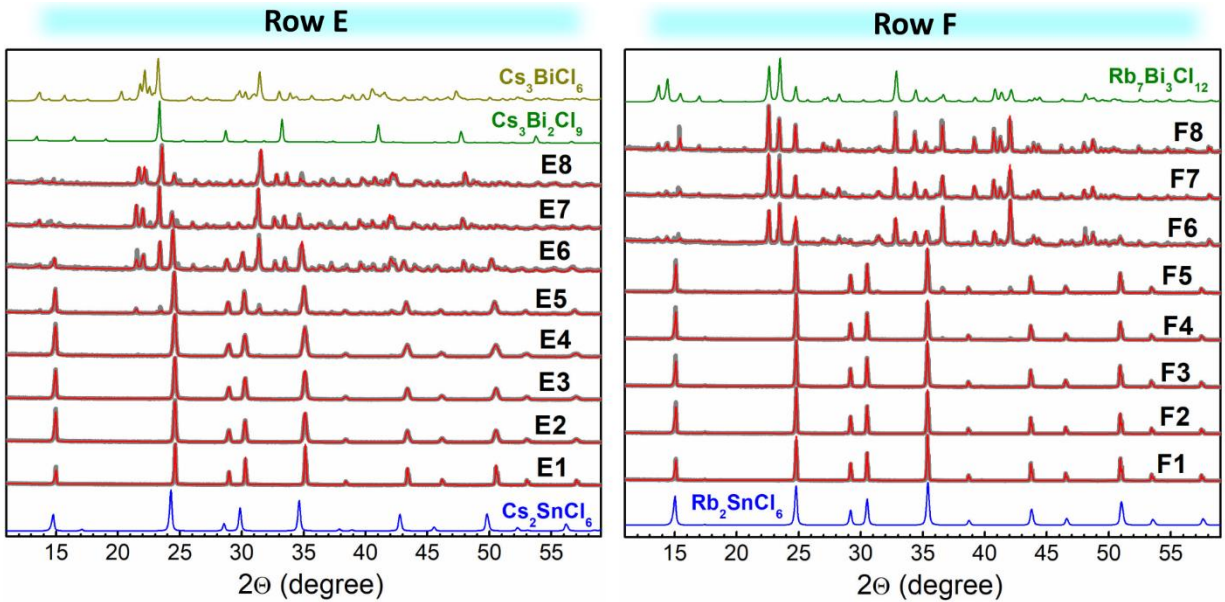


Figure S8. Powder X-ray diffraction patterns of $(\text{Cs}_x\text{Rb}_{1-x})_2\text{Sn}_y\text{Bi}_{1-y}\text{Cl}_6$ products in rows E and F. Gray lines show experimental diffractograms, red lines – Rietveld refinement. Calculated XRD profiles of single phases used for the refinements are presented along with experimental data.

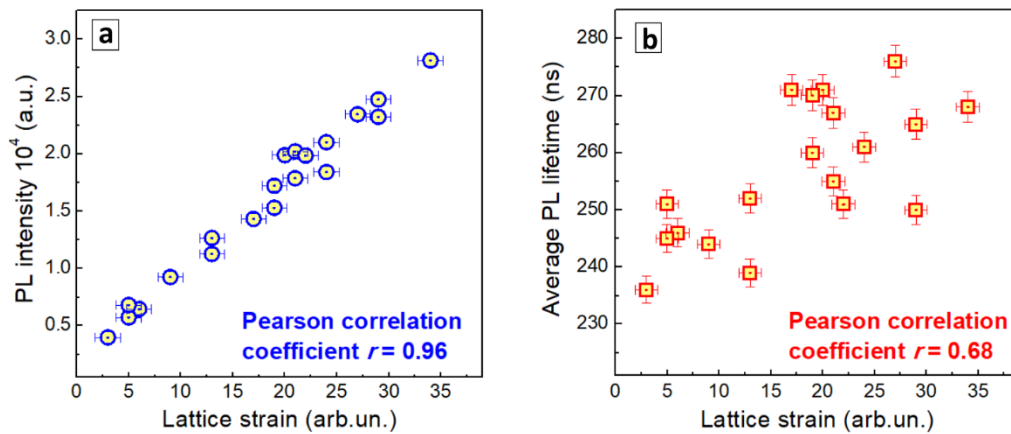


Figure S9. Correlations between the integral PL intensity (a) and PL lifetime (b) and lattice strain in the single-phase $(\text{Cs}_x\text{Rb}_{1-x})_2\text{Sn}_y\text{Bi}_{1-y}\text{Cl}_6$ products.

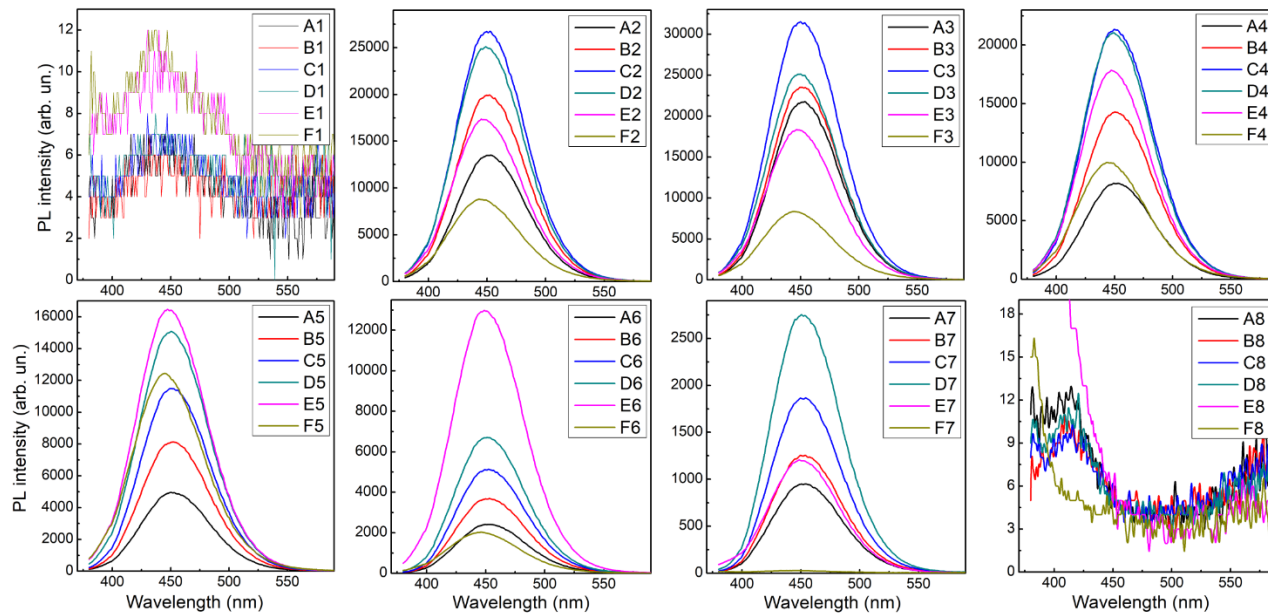


Figure S10. The complete collection of PL spectra of the $(\text{Cs}_x\text{Rb}_{1-x})_2\text{Sn}_y\text{Bi}_{1-y}\text{Cl}_6$ sample plate (PL excitation at 345 nm).

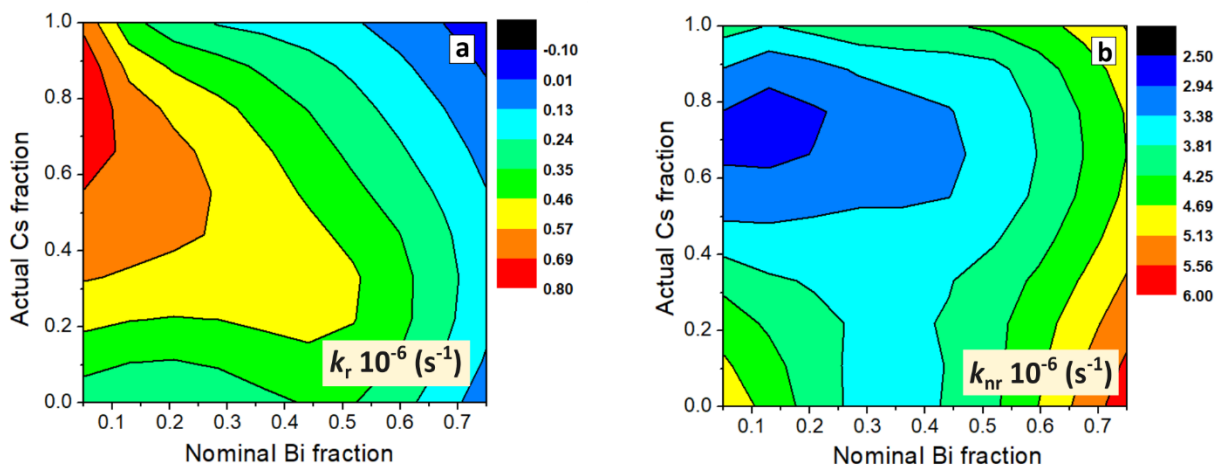


Figure S11. Compositional dependences of rate constant of radiative (k_r) and non-radiative (k_{nr}) recombination for the single-phase $(\text{Cs}_x\text{Rb}_{1-x})_2\text{Sn}_y\text{Bi}_{1-y}\text{Cl}_6$ products ($x = 0..1.0$, $y = 0.75..1.00$).